

The Pyrolysis of Azetidine: Shock-Tube Kinetics Similarities and Contrasts with Two Analogs

Y-X. ZHANG, C-L. YU, S. H. BAUER

Department of Chemistry, Baker Chemical Laboratory, Cornell University, Ithaca, New York 14853

Received 1 May 1997; accepted 30 June 1997

ABSTRACT: The kinetics of decomposition of azetidine $\{(CH_2)_3N-H\}$ was measured using single-pulse shock-tube techniques, over the temperature range 855–1100 K, in high argon dilution. These data confirm and extend an earlier investigation that utilized the very low-pressure pyrolysis method. A brief survey of many reports regarding the interesting features of azetidine is presented. In two appendices the thermodynamic and kinetic data on trimethylene sulfide, oxide, and immine are intercompared. New ab-initio calculations are cited for the parent species and their fragmentation products. © 1998 John Wiley & Sons, Inc. *Int J Chem Kinet* **30**: 185–191, 1998.

INTRODUCTION

The structure, thermochemistry, and molecular dynamics of fragmentation of four-member rings with the composition $(H_2C)_3X$, ($X = S, O, NH$) have received extensive study during the past decades. While our current interest is directed to azetidine ($X = NH$), because it is the core compounds for the tri-nitro substituted species {TNAZ}, we found it instructive to assemble the available experimental and computa-

tional data for the three listed species, to obtain estimates of how well ab-initio calculations agree with experiments for such structures. Our shock-tube results served to confirm and extend the kinetics of pyrolysis reported by Kamo et al. [1(a)] who used the VLPP technique.

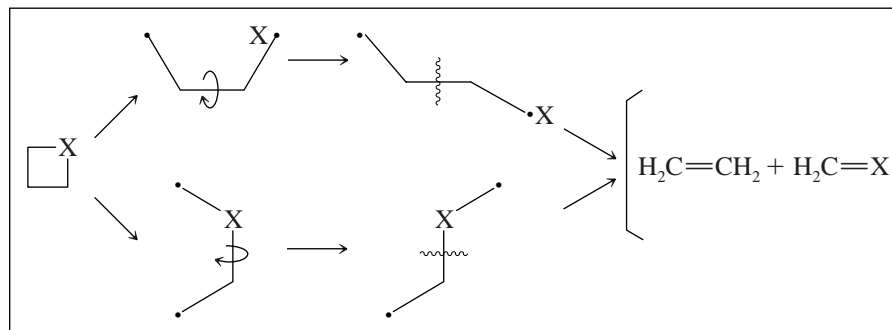
For the parent species the published data are assembled in Appendix A. The most plausible route for dissociation passes through biradical intermediates, generated when one bond in the ring is disrupted. That is the major activation step. The overall activation energies range from 54.8 to 65 kcal/mol. The overall entropy of activation (ΔS^\ddagger) arises primarily from the large amplitude motion about the bond opposite to the broken one and the increased loosening of the second bond prior to breaking.

Correspondence to: S. H. Bauer

Contract grant Sponsor: Army Research Office

Contract grant number: Grant # DAAH 04-95-1

© 1998 John Wiley & Sons, Inc. CCC 0538-8066/98/030185-07



Scheme I

Since the first step in the pyrolysis of the ring generates $\text{H}_2\text{C}=\text{CH}_2$ and $\text{H}_2\text{C}=\text{X}$, we focused on establishing the fate of the $\text{H}_2\text{C}=\text{X}$ species, to determine whether these products, at about 1000 K, remain intact or fragment to produce reactive radicals that could attack the parent compound or the ethylene. In Appendix B we summarized published experimental magnitudes and recently derived ab-initio estimates (via CBS-4). It appears that the activation energies for fragmentation of $\text{H}_2\text{C}=\text{X}$ range from ca. 80 to 90 kcal/mol; for AZ only a rough estimate is available. The derived k_{uni} at 1000 K is ca. $4 \times 10^{-5} \text{ s}^{-1}$, so that the corresponding half-times are several orders of magnitude longer than the residence time in our reactor. Volkova et al. [1(b)] reported that $\text{H}_2\text{C}=\text{NH}$ did decompose in a low pressure pyrolysis unit. (ca. 3×10^{-3} torr, 400–700°C).

COMMENTS ON AZETIDINE

The gas-phase structure was determined by electron diffraction and microwave spectroscopy [2]. The equatorial position of H(N) was confirmed as the dominate conformation. In the gas phase the interatomic distances in the ring of AZ differ somewhat from those in the crystalline solid and particularly from solid trinitro-azetidine. So does the flap angle [3]. The vibrational frequencies were remeasured, and with suitable scaling were reproduced by ab-initio calculations at the 6–31G* level [4]. The inversion rate at the N atom was estimated from temperature-dependent NMR line-width measurement; $\Delta H^\ddagger = 5.0 \text{ kcal/mol}$ and $\Delta S^\ddagger = -10.8 \text{ eu}$ [5]. Ab-initio calculations by these investigators, at the MP3 level indicated a barrier height of 6.48 kcal. (At the same level, the derived inversion barrier for ammonia was found to be 5.33 kcal, compared with the microwave value of 5.93 [6]). An earlier theoretical analysis [7] using STO-3G led to a

much higher barrier. A recent calculation at the CBS-4 level [8] for the enthalpy difference between the ground state conformation of AZ and the planar transition structure {for the heavy atoms and H(N)} found 5.57 kcal/mol. The low-frequency IR and Raman spectra were accounted for by an unsymmetrical potential well for the flapping motion of the ring atoms, with no second well for an axial H(N) [9]. The shoulder in the potential energy function appears between the flapping vibrational levels 3 and 4. Indeed, the CBS-4 calculation [8] for a structure initially constrained near the axial position, at an excitation of 1.65 kcal, showed no local minimum. However, later microwave spectra suggest that there may be a very shallow minimum at the location of the shoulder [10].

The vacuum UV absorption spectrum of AZ was recorded by Clark and Pickett [11]. Also, Clary and Henshaw [12(a)] suggested, on the basis of a theoretical analysis, that inversion at the N atom in AZ would be induced by intense laser radiation. Electron impact spectra of azetidine were recorded by Gallegor and Kiser [12(b)].

SHOCK-TUBE EXPERIMENTS

The shock tube is of stainless steel with a 1 inch inner diameter. The lengths of the driver and driven sections are 120 cm and 170 cm, respectively. A damping tank is attached to the driven section, next to the diaphragm holder. Shock waves were generated by increasing the pressure of the He driver until the mylar diaphragm broke. Typical pressures on the driver and driven sides are 80 psig and 300–400 torr, respectively. Two piezo-electric pressure sensors are stationed 10 cm apart at the end of the driven section. Their summed signal was recorded and digitized through Biomation 8100 and Northern Tracor Signal Analyzer, and then

stored in an IBM AT computer. The accuracy of the timed interval is $\pm 1 \mu\text{s}$, which corresponds to $\pm 8 \text{ K}$. The temperature in the reflected shock region was evaluated according to the computational procedure recommended by Gardiner et al [13] for very dilute reaction mixtures, and the shock-tube code developed by Mitchell and Kee (Sandia National Laboratory). Identical results were obtained from the above two algorithms for the mixtures used in experiments. The effective heating time (ca. 1.3 ms) was defined as the time elapsed from the beginning of the reflected shock wave to the point where the pressure signal was 80% of that in the reflected shock region. The storage tank, gas handling line, and the shock-tube were maintained at ca. 80°C throughout the experiments. Azetidine (>98% purity) from Aldrich was used without further purification. High purity Helium and Argon were used for the driving and carrier gases, respectively. Research grade ethylene, cyclopropane, and propene for GC calibration, are all from Matheson. (Caution: AZ rapidly attacks neoprene oh rings. All exposed plastic material was replaced with Teflon).

Immediately after each shock, a 16 ml of sample was collected through the sampling valve at the end of the driven section and analyzed in a Nicolet GC/9630 unit, using FID. To separate AZ from its reaction products a packed GC CarboGraph I column (from Alltech) was used. Injector and detector temperature were

TABLE I Parameters Used in RRKM Calculations

$E_0 = 52.0, \text{ kcal/mol}$					
Reaction path degeneracy 2					
Vibrational frequencies in molecule(cm^{-1})					
3357.7					
3003.2	2960.0	2931.6	2928.1	2861.9	2859.4
1498.7	1473.7	1450.1	1361.1	1320.5	1256.0
1250.9	1195.9	1174.8	1145.5	1082.8	
1028.2	990.5	948.8	928.1		
910.4	802.1	736.4	647.9		
217.0					
Vibrational frequencies in complex(cm^{-1})					
3357.7					
3003.2	2960.0	2931.6	2928.1	2861.9	2859.4
1498.7	1473.7	1450.1	1361.1	1320.5	1256.0
1250.9	1195.9	1174.8	1145.5	1082.8	
928.1	802.1	736.4	527.57		
486.83	467.13	332.44			
111.34					
Collision efficiency 1					
Collision cross section 5.0 Å					
Rotational constants A,B,C: 11.4487, 11.3366, 6.6090 (GHz)					

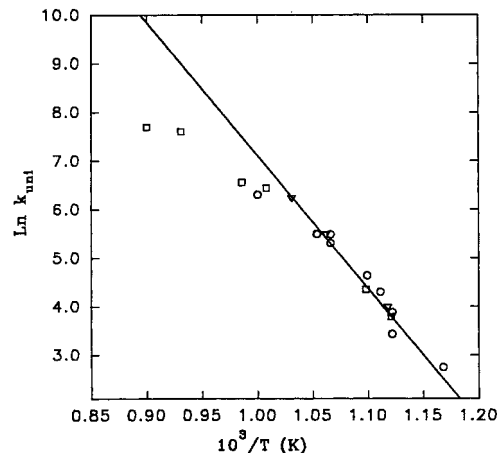


Figure 1 Unimolecular rate constants observed: (\square) 0.02% (mole fraction percentage); (∇) 0.03%, and (\circ) 0.19% azetidine in Ar. $P_5 = 5.0$ –6.3 atm. The line was calculated via RRKM using the parameters listed in Table I. $P_5 = 5.0$ atm.

typically set at 220°C and 250°C, respectively. The column temperature was set at 80°C for the first six minutes at then increased at a rate of 10°C/min until it reached the temperature of 275°C. The carrier gas flow rate was typically ca. 25 ml/min. The chromatograms were recorded with a Hewlett-Packard 3396A Integrator.

Azetidine, ethylene, and acetylene (above 1200 K) were identified and well separated by the above column under the specified operational conditions. Typical retention times for these compounds 14 min, 4 min, and 2.8 min, respectively. $\text{CH}_2=\text{NH}$ is an expected product but it was not observed in the above

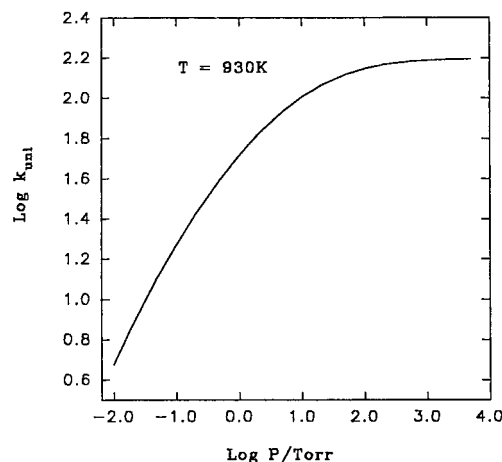


Figure 2 The computed fall-off curve at 930 K.

analysis. There are indications that it is destroyed or absorbed on the GC packing material.

First-order rate constants of the reaction were estimated from measured GC peak areas of azetidine and ethylene, respectively, with the following formula: $k_{\text{uni}} = \ln\{[AZ]_0/[AZ]_t\}/\Delta t = \ln\{[C_2H_4]^\infty/[C_2H_4]^\infty - [C_2H_4]_t\}/\Delta t$, where $[AZ]_t$ and $\{[C_2H_4]_t\}$ were obtained from the GC peak areas of azetidine and ethylene in the postshock mixture, $[AZ]_0$ from the GC peak area of the preshocked mixture, and $[C_2H_4]^\infty$ from the GC peak area of postshock mixture at high temperatures where all azetidine had decomposed. Δt is the heating time. Although the two methods gave almost identical results, it was found that rate constants obtained from azetidine peaks had a larger scatter, presumably due to variable losses of azetidine by wall absorption during sample transfers. Therefore, the final rate constants were determined from peak areas of C_2H_4 .

RESULTS

The temperature range covered was 855–1300 K. Below 1200 K C_2H_4 was the only reaction product. At higher temperatures, C_2H_2 was formed, presumably from subsequent decomposition of ethylene. The AZ fragmentation appears to be a clean unimolecular process. A least-squares fit to the experimental data up to 60% conversion (850–970 K) gave $k_u^\infty = 1.20 \times 10^{15} \exp(-54800 \pm 4200)/RT$, s^{-1} . For conversions greater than 60% the experimental points fall below the least-squares line, a “bend-over” typically observed for similar pyrolyses (cf. pyrrolidine [14]).

An RRKM calculation was performed with the parameters listed in Table I. The resulting line, drawn

through the measured rate constants is illustrated in Figure 1. That led to

$$k_u^\infty = 1.03 \times 10^{15} \exp(-54800/RT), s^{-1}.$$

The fall-off curve (at 930 K) is shown in Figure 2. An extended analysis of this aspect in the conversion of cyclic hydrocarbons was presented by Lin and Laidler [15]. In our analysis we assumed that ring opening occurs primarily by breaking a C—N bond. This is justified because the excitation energy required to break a C—C bond in a four-member ring, as in the cyclobutane, is about 10 kcal/mol higher than that observed for AZ (refer to Appendix A).

CONCLUSION

Shock-tube pyrolysis experiments confirmed and extended kinetic data on the fragmentation of azetidine. Tabular summaries are presented of the available thermochemical parameters for AZ and its analogs, trimethylene oxide and sulfide, supplemented with ab-initio calculations (at CBS-4 level). The decomposition pathways for the products generated upon the initial fragmentation of the ring structures were also summarized. We found no correlation between the magnitudes of the large amplitude flapping motions of the rings and the corresponding activation energies for ring fission.

This investigation was supported by the Army Research Office under Grant # DAAH 04-95-1, which we gratefully acknowledge.

APPENDIX A

APPENDIX A Table and References

Species	$\Delta H_f^\circ(298)$ kcal/mol	$S^\circ(298)$ eu	 \rightarrow dDH _r	$C_2H_4 + H_2CX$ δS_r	$k_u(T), s^{-1}$	Flap Angle	Barrier to Inversion kcal/mol
	14.48 ¹	67.54 ²	25.43(298) 24.87(900)	40.23 39.74	$2 \times 10^{15} \exp(-57000/RT)^{6a}$ $1 \times 10^{14} \exp(-52000/RT)^{6b}$	26 ⁹⁷	0.78 ⁸
H ₂ C=S	27.41 ³	55.22 ⁴					
H ₂ C=CH ₂	12.5 ⁵	52.40 ⁵					
	-19.25 ⁵	65.5 ⁵	5.80(298) 5.97(900)	39.21 40.23	$2.63 \times 10^{15} \exp(-62000/RT)^{9a}$ $5.13 \times 10^{15} \exp(-63000/RT)^{9b}$	large amp motion about 0	0.044 ^{8,10}
H ₂ C=O	-25.95 ⁵	52.3 ⁵					
	6.79 ⁵	63.2 ⁵	18.21(298) 18.24(900)	41.58 42.26	$3.98 \times 10^{15} \exp(-62500/RT)^{11}$	27.9 ¹²	1.46 ¹²
	23.47 ¹³	63.9 ¹⁴	11.93(298) 11.48(900)	41.50 41.28	$2.51 \times 10^{15} \exp(-55600/RT)^{13}$ $9.54 \times 10^{14} \exp(-54800/RT)^{16}$	29.7 ^{14b}	5.0 ^{14a}
H ₂ C=N-H	22.9 ^{5,15}	52.96 ⁵					

¹ J. B. Pedley, R. D. Naylor, and S. P. Kirby, *Thermochemical Data of Organic Compounds*, Chapman and Hall, London, 1986, 2nd ed.

² Calculated from molecular structure and vibrational frequencies. (a) C. T. Nielser, *Acta Chem. Scand.* **A31**, 791 (1997), (b) R. A. Shaw, C. Castro, N. Ibrahim, and H. Wieser, *J. Phys. Chem.*, **92**, 6528 (1988).

³ B. Ruscic and J. Berkowitz, *J. Chem. Phys.*, **98**, 2568 (1993).

⁴ Calculated from molecular constants, cited by M. Jacox, *J. Phys. Chem. Ref. Data.* **17**, 269 (1988).

⁵ Polynomial sets listed in *Tables of Thermofunctions*—A. Burcat, B. McBride, Technion-Areospace Eng. Report (1996).

⁶ (a) M. Yamada, et al. *Nippon Kagaku Kaishi* **59**, 870 (1987). (b) P. Jeffers, C. Dasch, S. H. Bauer, *Int. J. Chem. Kinet.* **5**, 545 (1973).

⁷ K. Karakida, K. Kuchitsu, *Bull. Chem. Soc. Japan* **48**, 1691 (1975).

⁸ L. A. Carreira, R. C. Lord, T. B. Malloy, Jr. in *Topics in Current Chem.* Vol. 82. Springer-Verlag, Berlin, 1979.

⁹ (a) L. Zalotai, et al. *Int. J. Chem. Kinet.* **15**, 505 (1983). (b) K. A. Holbrook, R. A. Scott, *J. Chem. Soc. Faraday Trans.* **71**, 1849 (1975).

¹⁰ S. Chan, et al. *J. Chem. Phys.* **44**, 1103 (1966).

¹¹ D. R. Lewis, et al. *J. Phys. Chem.* **88**, 4112 (1984).

¹² T. Egawa, et al. *J. Chem. Phys.* **86**, 6018 (1987).

¹³ T. Kamo, M. Yamada, J. Tang, Y. Ohshima, *Nippon Kagaku Kaishi* **8**, 1560 (1987).

¹⁴ Calculated from molecular constants, cited by (a), R. Dutler, A. Rauk, R. A. Shaw, *J. Phys. Chem.* **94**, 118 (1990). (b) H. Gunther, G. Schrem, H. Oherhammer, *J. Mol. Spec.* **104**, 152 (1984).

¹⁵ $\Delta H_f^\circ(H_2C=NH)$ is controversial; proposed values range from 16-26 kcal/mol.

¹⁶ This report.

APPENDIX B

In the attached tables we summarized the thermochemical constraints that control the fragmentation of the species $H_2C = X$ ($X = S, O, NH$) that are generated upon dissociation of the corresponding four-member rings. For eleven of the 18 species that are included, NASA format polynomials are available: (Burcat and McBride, Technion report, 1996). For the remaining seven $\{C_3H_6S(c); C_3H_6NH(c); H_2CS; HCS; H_2CN; HCNH(tr); HCNH(cis)\}$ the enthalpies of formation, structures, and vibrational frequencies were assembled from various reports, and their thermochemical functions were computed for a wide range of temperatures. These were then fitted to standard polynomials (available upon request). In Table B1 we listed the derived enthalpies of formation (kcal/mol) and standard entropies (eu, ideal gas phase) for the seven species. A wide range of values were reported for the enthalpy of formation of H_2CNH , ranging from 16.5 to 26.4; we chose 22.9 kcal, as accepted by Burcat and McBride. Values for the other species in that family are consistent with that magnitude. Table B2 is a compilation of enthalpy and entropy increments for a sequence of interconversions at 298 K and 900 K. The cited activation energies were estimated on the basis of analogy with the two measured rate constants.

TABLE B1

Species	ΔH_f° kcal/mol (298.15 K)	S° e.u. (298.15 K)	C_p cal/mol-K
$C_3H_6S(c)$	14.48 ²	67.34	16.78
$H_2C=S$	27.41 ³	55.22	9.12
HCS	71.82 ⁴	56.43	8.86
$C_3H_6NH(c)$	23.47 ⁵	63.84	15.98
$H_2C=NH$	22.9 ¹	52.96 ¹	9.10 ¹
H_2CN	57.40 ⁶	53.58	9.02
HCNH(tr)	71.40 ⁶	54.71	9.09
HCNH(cis)	76.40 ⁶	54.82	9.29

¹ A. Burcat, B. McBride, *Technion-Areospace Eng. Report.* (1996).

² J. B. Pedley, R. D. Naylon, and S. P. Kirby, *Thermochemical Data of Organic Compounds*, 2nd ed. Chapman and Hall, London, 1986, AND—Calculations based on molecular structure and vibrational frequencies reported by Nielser and Shaw (see ref. 2, APP.A)

³ B. Ruscic and J. Berkowitz, *J. Chem. Phys.*, **98**, 2568 (1993), AND—Calculations based on data compiled by M. Jacox, *J. Phys. Chem. Ref. Data.* **17**, 269 (1988).

⁴ Ref. 3 above, and J. Senekowitch, S. Carter, P. Rosmur, H-J. Werner, *Chem. Phys.* **147**, 281 (1990).

⁵ T. Kamo, et al. Ref. 13; Dutler, et al., Ref. 14, APP.A

⁶ Calculated from data cited in: (a) K. L. Nesbit, et al. *J. Phys. Chem.* **95**, 7613 (1991). (b) R. A. Bair, T. H. Dunning, *J. Chem. Phys.* **82**, 2280 (1985).

Table B2 Thermodynamical Increments Upon Reaction. Values in kcal/mol and e.u. at 298.15 K and 900 K

Reaction	ΔH_r°	ΔS_r°	E_a (estm)
R1. $H_2CS \longrightarrow H_2 + CS$	39.59(298) 41.10(900)	26.31 29.51	97
R2. $H_2CS \longrightarrow H + HCS$	96.51(298) 98.38(900)	28.63 32.37	99
R3. $HCS \longrightarrow H + CS$	47.28(298) 48.68(900)	21.29 23.98	48
R4. $H_2CO \longrightarrow H_2 + CO$	-0.47(298) 1.29(900)	26.19 29.19	ca. 77 (slightly less than R5)
R5. $H_2CO \longrightarrow H + HCO$	88.09(298) 90.08(900)	28.75 32.69	$k_{bi} = 1.26 \times 10^{16} \exp(77890/RT)$ cm ³ /mol.s (ref. 1)
R6. $HCO \longrightarrow H + CO$	15.65(298) 17.17(900)	21.04 24.06	18
R7. $H_2CNH \longrightarrow H_2 + HNC$	23.56(298) 26.08(900)	27.40 32.69	84
R8. $H_2CNH \longrightarrow H_2 + HCN$	9.37(298) 11.58(900)	26.51 31.14	85
R9. $H_2CNH \longrightarrow H + H_2CN$	86.60(298) 88.61(900)	28.04 32.04	86
R10. $H_2CNH \longrightarrow H + HCNH(tr)$	100.60(298) 102.71(900)	29.17 33.35	100

(Continued)

Table B2 (Continued)

R11. H ₂ CNH	→	H	+	HCNH(cis)	105.60(298)	29.28		106
					107.34(900)	33.71		
R12. HCN	→	HNC			14.19(298)	0.88	$k_u = 3.5 \times 10^{13} \exp(-47190/RT),$ s^{-1} (ref. 2)	
					14.5(900)	1.55		
R13. H ₂ CN	→	H	+	HCN	26.97(298)	22.07		30
					28.93(900)	25.94		
R14. HCNH(tr)	→	H	+	HNC	27.16(298)	21.83		30
					29.34(900)	26.18		
R15. HCNH(tr)	→	H	+	HCN	12.97(298)	20.95		30
					14.83(900)	24.63		

¹D. L. Baulch, *J. Phys. Chem. Ref. Data*, **21**, 411 (1992).

²M. C. Lin, Y. He, and C. F. Melius, *Int. J. Chem. Kinet.*, **24**, 1003 (1992).

BIBLIOGRAPHY

- (a) T. Kamo, M. Yamada, J. Tang, Y. Ohshima, and A. Amano, *Nippon Kagaku Kaishi*, **8**, 1560 (1987); (b) V. V. Volkova, et al. *Tetrahedron Lett.*, 577 (1978).
- H. Günther, G. Schrem, H. Oherhammer, *J. Mol. Spec.* **104**, 152 (1984).
- (a) T. C. Archibald, R. Gilardi, K. Baum, *J. Org. Chem.* **55**, 2920 (1990). (b) See also crystal structures by: P. Huszthy, et al. *Heterocyclic Chem.* **30**, 1197 (1993).
- R. Dutler, A. Rauk, R. A. Shaw, *J. Phys. Chem.* **94**, 118 (1990).
- R. Dutler, A. Rauk, T. S. Sorensen, *J. Am. Chem. Soc.* **109**, 3224 (1987).
- M. F. Maming, *J. Chem. Phys.* **3**, 136 (1935).
- J. Catalàn, O. Mo, M. Yàñez, *J. Mol. Str.* **43**, 251 (1978).
- C. F. Wilcox, Jr. Cornell University (unpublished).
- (a) L. A. Carreira, R. O. Carter, J. R. Durig, *J. Chem. Phys.* **57**, 3384 (1972); (b) A. G. Robiette, T. R. Bangers, H. L. Strauss, *Molecular Phys.* **42**, 1519 (1981).
- Ref. 2, p163.
- P. A. Clark, L. W. Pickett, *J. Chem. Phys.* **64**, 2060 (1976).
- (a) D. C. Clary, and J. P. Henshaw, *J. Phys. Chem.*, **87**, 3025 (1983); (b) E. J. Gallegos, R. W. Kiser, *J. Phys. Chem.*, **66**, 136 (1962).
- W. C. Gardiner, Jr., and B. F. Walker, and C. B. Wakefield, in *Shock Waves in Chemistry*, A. Lifshitz, Ed., Marcel Dekker, New York, 1981, Chap. 7.
- A. Lifshitz, M. Bidani, A. Agranat, A. Suslensky, *J. Phys. Chem.* **91**, 6043 (1987).
- M. C. Lin, K. J. Laidler, *Trans. Faraday Soc.* **64**, 927 (1968).

